

Closed-shell properties of ^{24}O with *ab initio* coupled-cluster theory

Ø. Jensen,^{1,2} G. Hagen,^{3,4} M. Hjorth-Jensen,² and J. S. Vaagen¹

¹*Department of Physics and Technology, University of Bergen, N-5007 Bergen, Norway*

²*Department of Physics and Center of Mathematics for Applications, University of Oslo, N-0316 Oslo, Norway*

³*Physics Division, Oak Ridge National Laboratory, Oak Ridge, Tennessee 37831, USA*

⁴*Department of Physics and Astronomy, University of Tennessee, Knoxville, Tennessee 37996, USA*

(Received 27 December 2010; published 22 February 2011)

We present a microscopic calculation of spectroscopic factors for neutron and proton removal from ^{24}O using the coupled-cluster method and a state-of-the-art chiral nucleon-nucleon interaction at next-to-next-to-next-to-leading order. To account for the coupling to the scattering continuum we use a Berggren single-particle basis that treats bound, resonant, and continuum states on an equal footing. We report neutron removal spectroscopic factors for the ^{23}O states $J^\pi = 1/2^+, 5/2^+, 3/2^-$, and $1/2^-$ and proton removal spectroscopic factors for the ^{23}N states $1/2^-$ and $3/2^-$. Our calculations support the accumulated experimental evidence that ^{24}O is a closed-shell nucleus.

DOI: [10.1103/PhysRevC.83.021305](https://doi.org/10.1103/PhysRevC.83.021305)

PACS number(s): 21.10.Jx, 21.60.De, 21.10.Pc, 31.15.bw

Introduction. The study of nuclei far from stability is a leading direction in nuclear physics, experimentally and theoretically. It represents a considerable intellectual challenge to our understanding of the stability of matter itself, with potential implications for the synthesis of elements. An important aspect of this research direction is to understand how magic numbers and shells appear and evolve with increasing numbers of neutrons or protons. The structure and properties of barely stable nuclei at the limits of stability have been demonstrated to deviate dramatically from the established patterns for ordinary and stable nuclei (see Ref. [1] and references therein for a recent review). One of the striking features of nuclei close to the drip line is the adjustment of shell gaps, giving rise to different *magic numbers* [2]. The way shell closures and single-particle properties evolve as functions of the number of nucleons forms one of the greatest challenges to our understanding of the basic features of nuclei and thereby the stability of matter.

The chain of oxygen isotopes up to ^{28}O is particularly interesting because these are the heaviest nuclei for which the drip line is well established. Two out of four stable even-even isotopes exhibit a doubly magic nature, namely ^{22}O ($Z = 8$, $N = 14$) and ^{24}O ($Z = 8$, $N = 16$). Several recent experiments [3–6] provide evidence that ^{24}O is the last stable oxygen isotope. This is remarkable, in particular if one considers the fact that the addition of a single proton on top of the $Z = 8$ closed shell brings the drip line of the fluorine isotopes to ^{31}F . Recent measurements [3] also suggest that ^{24}O has a spherical neutron configuration. The isotopes $^{25-28}\text{O}$ are all believed to be unstable toward neutron emission, even though ^{28}O is a doubly magic nucleus within the standard shell-model picture. This indicates that the magic number at the neutron drip line for the oxygen isotopes is not at $N = 20$ but rather at $N = 16$.

Although spectroscopic factors are not observable quantities [7,8], they can be used to address shell closure properties within the context of a given model. Experimentally, spectroscopic factors are defined as the ratio of the observed

reaction rate with respect to the same rate, calculated with a particular reaction model and assuming a full occupation of the relevant single-particle states. The spectroscopic factors are then interpreted as the occupancy of specific single-particle states. Theoretically, however, spectroscopic factors measure what fraction of the full wave function corresponds to the product of a correlated state (often chosen to be a given closed-shell core) and an independent single-particle or single-hole state. Large deviations from the values predicted by an independent-particle model point to a strongly correlated system.

Kanungo *et al.* [3] reported measurements of one-neutron removal from ^{24}O and an extraction of spectroscopic factors. They used an eikonal reaction model and Woods-Saxon overlap functions, which were calculated with a well depth adjusted to reproduce the one-neutron separation energies. The results were compared with shell-model predictions using the phenomenological *sd*-shell interaction, version B of Ref. [9] and a fitted multi-shell interaction for the *sd* and *pf* shells [10]. The theoretical calculations corroborate the large *s*-wave probability found in the experimental analysis, implying thereby that ^{24}O is indeed a doubly magic nucleus.

The aim of this work is to add further theoretical evidence and support to these claims. We present spectroscopic factors for neutron and proton removal from ^{24}O as predicted by the coupled-cluster method with the chiral nucleon-nucleon interaction by Entem and Machleidt [11] at next-to-next-to-next-to-leading order (N^3LO). Our calculations are performed in a large single-particle basis which includes bound and continuum single-particle states. The aforementioned theoretical calculations of Refs. [9,10] involve only fitted effective interactions tailored to small shell-model spaces, such as the *sd* or the *sd-pf* shells only.

The virtue of *ab initio* methods applied to nuclear physics is to reduce the model dependence of computed results. By means of a recipe for systematic improvements, one can distinguish between parameters of technical and physical character. Whereas the result may be expected to depend on

physical parameters, it should be insensitive to the technical parameters as systematic improvements are included. Ultimately, a converged *ab initio* result may provide a rigorous test of the nuclear interaction model and the corresponding physical parameters. Because our single-particle basis contains continuum states, and therefore represents the correct asymptotic behavior, we are able to generate radial overlap functions for drip-line nuclei. This work paves therefore the way for neutron-knockout reactions with rich microscopic structure information.

After these introductory remarks, we briefly expose our calculational formalism as well as the choice of Hamiltonian and basis in the next sections. Following that, our results are presented. Conclusions and perspectives are drawn in the final section.

Method. The aim of this section is to give a short overview of the steps in our calculations. The coupled-cluster method [12–22] and the application to spectroscopic factors [23] have been presented in great detail elsewhere. Here we give only a brief summary of the concepts that enter the calculations leading to the results presented in this article.

The spectroscopic factor (SF) is the norm of the overlap function,

$$S_{A-1}^A(lj) = |O_{A-1}^A(lj; r)|^2 \quad (1)$$

$$O_{A-1}^A(lj; r) = \sum_n \langle A-1 || \tilde{a}_{nlj} || A \rangle \phi_{nlj}(r). \quad (2)$$

Here $O_{A-1}^A(lj; r)$ is the radial overlap function of the many-body wave functions for the two independent systems with A and $A-1$ particles, respectively. The double bar denotes a reduced matrix element, and the integral-sum over n represents both the sum over the discrete spectrum and an integral over the corresponding continuum part of the spectrum. The annihilation operator \tilde{a}_{nljm} transforms like a spherical tensor of rank j and projection m . The radial single-particle basis function is given by the term $\phi_{nlj}(r)$, where l and j denote the single-particle orbital and angular momentum, respectively, and n is the nodal quantum number. The isospin quantum number has been suppressed. We emphasize that the overlap function, and hence also its norm, is defined microscopically and independently of the single-particle basis. It is uniquely determined by the many-body wave functions $|A\rangle$ and $|A-1\rangle$. The quality of the SF estimate is thus limited by the quality of the pertinent many-body wave functions.

Our calculation of SFs follows the recipe detailed in Ref. [23]. The important difference between this work and Ref. [23] is that all terms contributing to the SFs have now been expressed in terms of reduced matrix elements in an angular momentum coupled basis. This allows us to handle a much larger set of single-particle states, as discussed in Refs. [18,21].

We use the coupled-cluster ansatz, $|\psi_0\rangle = \exp(T)|\phi_0\rangle$ for the ground state of the closed-shell nucleus ^{24}O . The reference state, $|\phi_0\rangle$, is an antisymmetric product state for all A nucleons. The cluster operator T introduces correlations as a linear combination of particle-hole excitations $T = T_1 + T_2 + \dots + T_A$, where T_n represents an n -particle- n -hole excitation operator. For the coupled-cluster singles and doubles (CCSD)

approximation employed in this work, T is truncated at the level of double excitations, $T = T_1 + T_2$. The coupled-cluster solution for ^{24}O is obtained as a set of amplitudes that defines T .

Owing to the non-Hermiticity of the standard coupled-cluster ansatz, we need both the left eigenvectors and the right eigenvectors. These are determined via the equation-of-motion coupled-cluster (EOM-CC) approach as $|A\rangle \approx |R_v^A(J_A)\rangle \equiv \exp(T)R_v^A(J_A)|\phi_0\rangle$ and $\langle A| \approx \langle L_v^A(J_A)| \equiv \langle \phi_0|L_v^A(J_A)\exp(-T)$. The operators $R_v^A(J_A)$ and $L_v^A(J_A)$ produce linear combinations of particle-hole excited states when acting to the right and left, respectively. In the spherical form of the EOM-CC approach, the operators have well-defined angular momentum by construction, as indicated by J_A , which stands for the angular momentum considered. See, for example, Ref. [21]. If the A -body system is in its ground state, the right EOM-CC wave function is identical to the coupled-cluster ground state.

Solutions for the $A-1$ -body system, ^{23}O and ^{23}N , are obtained with particle-removal equations of motion (PR-EOM-CCSD), where we use the CCSD ground-state solution of ^{24}O as the reference state to determine the corresponding left and right eigenvectors as $|A-1\rangle \approx |R_\mu^{A-1}(J_{A-1})\rangle \equiv \exp(T)R_\mu^{A-1}(J_{A-1})|\phi_0\rangle$ and $\langle A-1| \approx \langle L_\mu^{A-1}(J_{A-1})| \equiv \langle \phi_0|L_\mu^{A-1}(J_{A-1})\exp(-T)$. In actual calculations, the EOM-CC wave functions are obtained by determining the operators $R_v^A(J_A)$ and $L_v^A(J_A)$ as eigenvectors of the similarity transformed Hamiltonian, $\bar{H} = \exp(-T)H\exp(T)$. The transformed Hamiltonian is non-Hermitian, which implies that the left eigenstates must be determined independently. We refer the reader to Refs. [14,20] for details about the equation-of-motion approach combined with coupled-cluster theory.

Finally, we can approximate the SF [Eq. (1)] in the spherical coupled-cluster formalism as

$$S_{A-1}^A(lj) = \sum_n \langle L_\mu^{A-1}(J_{A-1}) || \tilde{a}_{nlj} || R_v^A(J_A) \rangle \times \langle R_\mu^{A-1}(J_{A-1}) || \tilde{a}_{nlj} || L_v^A(J_A) \rangle^*, \quad (3)$$

where we have used the similarity transformed spherical annihilation operator as

$$\tilde{a}_{nljm} = \exp(-T)\tilde{a}_{nljm}\exp(T).$$

Closed expressions for the similarity transformed operators are given in Ref. [23]. The labels μ and ν are included to distinguish excited states of the (PR-)EOM-CC solutions. In the spherical formulation of EOM-CCSD, the solutions are spherical tensors [21], and the SF depends on the rank, but not on the projection of the EOM-CCSD states. To derive the coupled expressions, a Racah algebra module was developed for the open-source computer algebra system SYMPY [24]. More details about these calculations can be found in Ref. [25].

Hamiltonian and basis. We use an intrinsic A -nucleon Hamiltonian $\hat{H} = \hat{T} - \hat{T}_{\text{cm}} + \hat{V}$, where \hat{T} is the kinetic energy, \hat{T}_{cm} is the kinetic energy of the center-of-mass coordinate, and \hat{V} is the two-body nucleon-nucleon interaction. Coupled-cluster calculations starting from this Hamiltonian have been shown to generate solutions that are separable into a Gaussian

center-of-mass wave function and an intrinsic wave function (see, for example, Refs. [21,26] for further details).

The nucleon-nucleon interaction we use is the chiral N^3LO interaction model of Entem and Machleidt [11]. Although the interaction has a cutoff $\Lambda = 500$ MeV, it still contains high-momentum modes, and one typically needs model spaces that comprise about 20 major oscillator shells to reach convergence for the ground states of selected oxygen and calcium isotopes (see, for example, Refs. [21,27] for a discussion). However, exploiting the spherical symmetry of the interaction and our coupled-cluster formalism, we can use model spaces that are large enough so that there is no need for a subsequent renormalization of the interaction.

Unknown short-range properties are parametrized by contact terms in the interaction. The corresponding low-energy constants are fit to reproduce low-energy nucleon-nucleon scattering. This implies that the short-range dynamics will be sensitive to the momentum cutoff. Because we are neglecting many-body forces such as three-body forces or more complicated terms, our results will, in general, depend, more or less, on the chosen cutoff of the nucleon-nucleon interaction model. Quantities that are sensitive to the short-range part of the wave functions, such as SFs, may depend strongly on the chosen cutoff. This is why even *ab initio* calculations of SFs must be considered as model dependent. Our results may be fully converged in terms of a given Hamiltonian and its parameters at a given level of many-body physics; however, employing another nucleon-nucleon interaction may lead to slightly different results because many-body terms beyond those represented by a two-body interaction can be very important. This is discussed in detail in Ref. [27].

We use a Gamow-Hartree-Fock (GHF) solution for the reference state, as detailed, for example, in Ref. [20]. These Hartree-Fock solutions were built from the standard harmonic oscillator (HO) basis combined with Woods-Saxon (WS) single-particle states for selected partial waves to properly reproduce effects of the continuum. The role of the continuum is expected to be important close to the drip line, as seen in Refs. [20,28–30]. For this purpose we use a Berggren representation [31] for the neutron $s_{1/2}$, $d_{3/2}$, and $d_{5/2}$ partial waves. This representation generalizes the standard completeness relation to the complex energy plane. In the Berggren basis, bound, resonant, and nonresonant continuum states are treated on an equal footing. The Berggren ensemble has been successfully used within the Gamow shell model (see, for example, Ref. [29] for a recent review) and in coupled-cluster calculations of energies and lifetimes in Refs. [20,22]. The Berggren basis is constructed by diagonalizing a one-body Hamiltonian with a spherical WS potential in a spherical plane-wave basis defined on a discretized contour in the complex momentum plane. We employ a total of 30 Gauss-Legendre mesh points along the contour for each of the $s_{1/2}$, $d_{3/2}$, and $d_{5/2}$ neutron partial waves. With 30 discretized single-particle states our results for the above single-particle states become independent of the choice of contour. For the choice of interaction that we use, the $1/2^+$ and $5/2^+$ states are fairly well bound with respect to ^{22}O [21,32]; therefore, it is sufficient to use a contour along the real energy

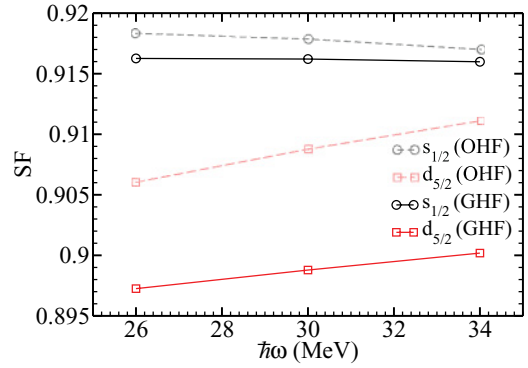


FIG. 1. (Color online) Normalized SFs plotted against $\hbar\omega$ for $J^\pi = 1/2^+$ and $5/2^+$ one-neutron removal from ^{24}O . The continuum states included in the Berggren-basis calculation (GHF) lead only to a small reduction compared with the harmonic oscillator values (OHF). The dependence on the oscillator spacing $\hbar\omega$ is very weak in both calculations. The inclusion of the continuum structure also gives a small, but visible, improvement in the $\hbar\omega$ dependence.

axis. For all other partial waves, the basis functions are those of the spherical HO.

Results. Figure 1 shows the SFs for removing a neutron in the $s_{1/2}$ and $d_{5/2}$ partial waves of ^{24}O as function of the HO frequency $\hbar\omega$. The ground-state $1/2^+$ and excited $5/2^+$ state in ^{23}O were calculated within the PR-EOM-CCSD approximation starting from the GHF basis with 30 mesh points for each of the $s_{1/2}$, $d_{3/2}$, and $d_{5/2}$ neutron partial waves and 17 major oscillator shells for the protons and remaining neutron partial waves. The SFs are well converged with respect to the model space size. To investigate the role of continuum on the SFs, we compare with a calculation done in a Hartree-Fock basis built from a HO basis of 17 major shells (OHF).

We find that the effect of the continuum is small. This is expected because our calculations of the $1/2^+$ and $5/2^+$ single-particle states in ^{24}O result in well bound states with respect to the neutron emission threshold, see for example Ref. [21] for more details. We do, however, see a small reduction of the SFs when the continuum is included. The reduction of SFs will be enhanced for states close to a reaction channel threshold as discussed in Ref. [33]. Although the

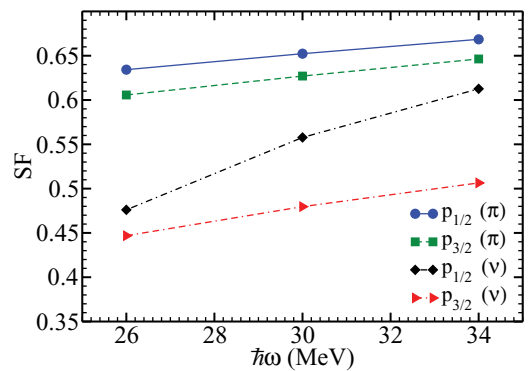


FIG. 2. (Color online) Normalized SFs plotted against $\hbar\omega$ for the negative parity states $J^\pi = 1/2^-$ and $3/2^-$ in one-proton (π) and one-neutron (ν) removal from ^{24}O .

effect of the continuum on the SFs is marginal in the cases we consider, the effect is crucial to obtain the correct asymptotic behavior of the overlap functions for one-neutron removal. It is the asymptotic normalization coefficient, which is calculated from the tail of the radial overlap function that enters the exact reaction amplitudes. It is arguably the relevant quantity to calculate for reactions [34]. The results in Fig. 1 show also that the SFs for the single neutron states close to the Fermi surface are close to one, indicating that a configuration consisting of a single-hole removal from ^{24}O captures much of the structure of the wave function for these states. The results for the neutron $s_{1/2}$ and $d_{5/2}$ hole states thus lend support to the accumulated evidence that ^{24}O can be interpreted as a closed-shell nucleus. For the proton states close to the Fermi surface, this finding is only partly corroborated by the results shown in Fig. 2. In that figure we show our results for the SFs for removing either a neutron or a proton in the $p_{3/2}$ and $p_{1/2}$ partial waves of ^{24}O . From Fig. 2 we see that the $3/2^-$ and $1/2^-$ states in neither ^{23}O nor ^{23}N can be clearly interpreted as simple one-hole states in ^{24}O . However, the stronger dependence on the HO frequency $\hbar\omega$ indicates that we are missing many-body correlations beyond the 2h-1p level in our PR-EOM-CCSD computations of the $1/2^-$ and $3/2^-$ states.

Our results for SFs and energies for the $J^\pi = 1/2^+, 5/2^+, 3/2^-, 1/2^-$ states in ^{23}O and the $J^\pi = 1/2^-, 3/2^-$ states in ^{23}N are summarized in Table I. We present the values that were calculated with a HO frequency $\hbar\omega = 30$ MeV, and the energies are given relative to the ground state of ^{23}O . The SFs agree with both the extracted value for the $1/2^+$ state and the theoretical results obtained with fitted shell-model interactions. The USDB interaction gives 1.810 for the neutron $1/2^+$ state and 5.665 for the neutron $5/2^+$ state. Corresponding numbers for SDFP-M are 1.769 and 5.593, respectively [3].

As can be seen from Table I, our spacing between the two one-hole states is only 0.35 MeV. This disagrees with the shell-model calculations with fitted interactions reported in Ref. [3]. The energy spacing is 2.586 and 2.593 MeV for the SDFP-M interaction and the USDB interaction, respectively. Assuming a large SF for the $5/2^+$ state, a bound $5/2^+$ -wave state at an energy consistent with the shell-model predictions should have been seen in the experiment of Kanungo *et al.* [3]. The lack of such an observation was interpreted as a confirmation that this state is unbound. We speculate that missing three-nucleon forces could play an important role regarding the shell gap between the $1/2^+$ and $5/2^+$ single-particle states in ^{24}O . However, recent shell-model calculations by Otsuka *et al.* [32], where three-body interactions were included at the normal-ordered two-body level, give a spacing between the $1/2^+$ and the $5/2^+$ single-particle states of ~ 0.55 MeV (dashed-dotted line in Fig. 2(d) of Ref. [32]), a result which is close to ours (see Table I). Calculations performed with different approaches to many-body perturbation theory, employing the same nucleon-nucleon interaction, produce qualitatively similar results as those reported here. Further investigations are thus needed to clarify the discrepancies between the results reported in, for example, Ref. [3] and the present results and those of Otsuka *et al.* [32]. Compared with the experimental results in Table I, we note that the experimental error bars are typically orders of

TABLE I. Energies for states in ^{23}O and ^{23}N and corresponding spectroscopic factors (SF) for the removal of a particle from ^{24}O . Note that the SFs are multiplied with the factor $2J + 1$. The reported coupled-cluster results are at the level of singles and doubles (CCSD) and are calculated with $\hbar\omega = 30$ MeV. Experimental values for ^{23}O are taken from Ref. [3] and data for ^{23}N are taken from Ref. [35].

		PR-EOM-CCSD		Experiment	
		E	SF	E	SF
^{23}O	$1/2^+$	0.0	1.832	0.0	1.71 ± 0.19
	$5/2^+$	0.35	5.393		
	$3/2^-$	12.4	1.919		
^{23}N	$1/2^-$	13.4	1.116		
	$3/2^-$	20.7	2.609		
	$1/2^-$	21.8	1.254	22.33	

magnitude larger than the dependence on technical parameters displayed in Figs. 1 and 2. Finally, we note that the $1/2^-$ state in ^{23}N is in very good agreement with the theoretical mass evaluations of Ref. [35].

However, there is still a considerable model dependence inherent in the calculation of SFs. First of all, our calculations have been performed at the level of the singles and doubles approach, meaning that all correlations up to the level of two-particle–two-hole excitations are included to infinite order. Some selected higher n -particle– n -hole correlations are also included. The inclusion of triples correlations, that is the admixture of three-particle–three-hole correlations on the ground state of the nucleus with A nucleons and 3h-2p excitations in the PR-EOM-CCM calculations of the $A - 1$ nucleus, on SFs remains to be investigated. The largest uncertainty in our calculations is, however, most likely the effect of three-body interactions arising in chiral perturbation theory. A recent analysis by Otsuka *et al.* [32] demonstrates in shell-model calculations constrained by the degrees of freedom of the sd shell, that three-body interactions are important to obtain the experimental trend in binding energies for the oxygen isotopes. Three-body interactions, included at the normal-ordered two-body level, result in ^{25}O as unbound with respect to ^{24}O . However, there are still open questions, as effects coming from coupling to the continuum and effective many-body forces induced by truncation of the Hamiltonian to the sd shell may play an important role. Inclusion of three-body interactions together with the effects of coupling to the continuum in coupled-cluster calculations of SFs and single-particle energies, is a topic for future investigations.

Conclusion and outlook. We have computed single-particle energies and SFs for hole states in ^{24}O using coupled-cluster theory at the level of singles and doubles correlations. The role of continuum states has also been included in our investigations. For the hole states the major influence of the continuum states is to give final single-particle energies and SFs which are almost independent of the chosen oscillator energy. The SFs for protons and neutrons obtained with microscopic coupled-cluster calculations support the emerging consensus that ^{24}O is a doubly magic nucleus. In future work we plan to investigate

the application of radial overlap functions to neutron knockout reactions on drip-line nuclei, thereby removing a level of model dependence from reaction studies.

Discussions with Gustav R. Jansen are acknowledged. This work was supported by the Office of Nuclear Physics,

US Department of Energy (Oak Ridge National Laboratory), and DE-FC02-07ER41457 (SciDAC UNEDF). This research used computational resources of the National Center for Computational Sciences and the Notur project in Norway. Ø.J. and M.H.J. acknowledge support from the Research Council of Norway (NFR 171247/V30).

-
- [1] M. Thoennessen, *Rep. Prog. Phys.* **67**, 1187 (2004).
 - [2] A. Ozawa, T. Kobayashi, T. Suzuki, K. Yoshida, and I. Tanihata, *Phys. Rev. Lett.* **84**, 5493 (2000).
 - [3] R. Kanungo *et al.*, *Phys. Rev. Lett.* **102**, 152501 (2009).
 - [4] M. Stanoiu *et al.*, *Phys. Rev. C* **69**, 034312 (2004).
 - [5] C. R. Hoffman *et al.*, *Phys. Lett. B* **672**, 17 (2009).
 - [6] W. N. Catford *et al.*, *Phys. Rev. Lett.* **104**, 192501 (2010).
 - [7] R. J. Furnstahl and H.-W. Hammer, *Phys. Lett. B* **531**, 203 (2002).
 - [8] R. J. Furnstahl and A. Schwenk, *J. Phys. G* **37**, 064005 (2010).
 - [9] B. A. Brown and W. A. Richter, *Phys. Rev. C* **74**, 034315 (2006).
 - [10] Y. Utsuno, T. Otsuka, T. Glasmacher, T. Mizusaki, and M. Honma, *Phys. Rev. C* **70**, 044307 (2004).
 - [11] D. R. Entem and R. Machleidt, *Phys. Rev. C* **68**, 041001(R) (2003).
 - [12] J. Čížek, *Adv. Chem. Phys.* **14**, 35 (1969).
 - [13] J. Čížek, *J. Chem. Phys.* **45**, 4256 (1966).
 - [14] R. J. Bartlett and M. Musiał, *Rev. Mod. Phys.* **79**, 291 (2007).
 - [15] F. Coester, *Nucl. Phys.* **7**, 421 (1958).
 - [16] F. Coester and H. Kümmel, *Nucl. Phys.* **17**, 477 (1960).
 - [17] D. J. Dean and M. Hjorth-Jensen, *Phys. Rev. C* **69**, 054320 (2004).
 - [18] G. Hagen, T. Papenbrock, D. J. Dean, and M. Hjorth-Jensen, *Phys. Rev. Lett.* **101**, 092502 (2008).
 - [19] G. Hagen, T. Papenbrock, D. J. Dean, M. Hjorth-Jensen, and B. Velamuri Asokan, *Phys. Rev. C* **80**, 021306(R) (2009).
 - [20] G. Hagen, T. Papenbrock, and M. Hjorth-Jensen, *Phys. Rev. Lett.* **104**, 182501 (2010).
 - [21] G. Hagen, T. Papenbrock, D. J. Dean, and M. Hjorth-Jensen, *Phys. Rev. C* **82**, 034330 (2010).
 - [22] G. Hagen, D. J. Dean, M. Hjorth-Jensen, and T. Papenbrock, *Phys. Lett. B* **656**, 169 (2007).
 - [23] Ø. Jensen, G. Hagen, T. Papenbrock, D. J. Dean, and J. S. Vaagen, *Phys. Rev. C* **82**, 014310 (2010).
 - [24] SymPy Development Team (2010), SymPy: Python library for symbolic mathematics [www.sympy.org].
 - [25] Ø. Jensen, Ph.D. thesis, University of Bergen, 2011.
 - [26] G. Hagen, T. Papenbrock, and D. J. Dean, *Phys. Rev. Lett.* **103**, 062503 (2009).
 - [27] M. Hjorth-Jensen, D. J. Dean, G. Hagen, and S. Kvaal, *J. Phys. G* **37**, 064035 (2010).
 - [28] K. Tsukiyama, M. Hjorth-Jensen, and G. Hagen, *Phys. Rev. C* **80**, 051301 (2009).
 - [29] N. Michel, W. Nazarewicz, M. Płoszajczak, and T. Vertse, *J. Phys. G* **36**, 013101 (2009).
 - [30] A. Volya and V. Zelevinsky, *Phys. Rev. C* **74**, 064314 (2006).
 - [31] T. Berggren, *Nucl. Phys. A* **109**, 265 (1968).
 - [32] T. Otsuka, T. Suzuki, J. D. Holt, A. Schwenk, and Y. Akaishi, *Phys. Rev. Lett.* **105**, 032501 (2010).
 - [33] N. Michel, W. Nazarewicz, and M. Płoszajczak, *Phys. Rev. C* **75**, 031301 (2007).
 - [34] A. M. Mukhamedzhanov and A. S. Kadyrov, *Phys. Rev. C* **82**, 051601(R) (2010).
 - [35] G. Audi, A. H. Wapstra, and C. Thibault, *Nucl. Phys. A* **729**, 337 (2003).